Dielectric Analysis of High-Density Polyethylene-Graphite Composites for Capacitor and EMI Shielding Application

Varij Panwar,[1] R. M. Mehra,[2] Jong-Oh Park,[1] Suk-ho Park[1]

[1]*School of Mechanical and Systems Engineering Chonnam National University, Gwangju 500-757, Republic of Korea*
[2]*School of Engineering and Technology, Sharda University, Knowledge Park 3, Greater Noida 201 306, Uttar Pradesh, India*

Received 31 October 2010; accepted 29 April 2011
DOI 10.1002/app.34818
Published online 6 February 2012 in Wiley Online Library (wileyonlinelibrary.com).

ABSTRACT: In this article, we present and analyze the dielectric properties of high-density polyethylene (HDPE)-graphite(Gr) composites in low and radio frequency ranges for capacitor and electromagnetic interference (EMI) shielding application, respectively. The HDPE-Gr composites were prepared by mixing and the hot compression mold technique. The dielectric constant and AC conductivity of HDPE-Gr composites according to graphite volume fraction follow the power law model of percolation theory. The percolation threshold of the composites was estimated to be 0.039 ($\sim$ 7 wt % of Gr). The HDPE-Gr composites exhibited high dielectric constants, high dissipation factors, and high AC conductivities at a certain addition of graphite in low frequency and radio frequency regions. The AC conductivity of the composites with the higher content of graphite depicted frequency independency in low and radio frequency region. The EMI shielding properties of the HDPE-Gr composites was evaluated in the radio frequency region and it was found that the maximum EMI shielding of the composites was obtained. © 2012 Wiley Periodicals, Inc. J Appl Polym Sci 125: E610–E619, 2012

Key words: dielectric properties; composites; polyethylene

INTRODUCTION

Conductive polymer composites can be fabricated by mixing an insulating polymer matrix with conductive fillers. Graphite powder,[1–4] carbon black,[5–8] metallic powder,[9,10] carbon nanotube,[11–13] piezoelectric powder[14,15] and carbon nanofiber (CNF)[16,17] have been used as conducting fillers. The advantages of using polymer and graphite in polymer composites include lighter weight, corrosion resistance, and easy processing and flexibility. Conducting polymer composites can be applied to current limiters,[18,19] charge storage capacitors[14,20,21] and antistatic materials, which can provide electromagnetic interference (EMI) shielding[22,23] for electronic devices.

The dielectric constant and AC conductivity of conducting polymer composites increase with the addition of the conducting filler. Especially, near the percolation threshold (ϕ_c), the dielectric constant and AC conductivity change sharply. At the ϕ_c, many conducting particles are isolated by thin insulating layers. Therefore, near the percolation threshold, the composites can become a capacitor and therefore, can be applied to charge storing devices, electro active polymers (EAP) and decoupling capacitor applications. Polymer composites of high dielectric constant and dissipation factor in low and high frequency regions are required for various applications, such as charge storage capacitors, decoupling capacitors and EMI shielding applications.

Electromagnetic radiation at radio and microwave frequencies such as those emanating from cell phones tends to interfere with electronic devices. Therefore, the EMI leakage in the radio to microwave frequency range is still a serious problem in our society. To control the EMI leakage, conducting polymer composites have been widely used in the area of EMI/radio-frequency interference (RFI) shielding effectiveness (SE) due to their unique combination of electrical conduction, corrosion resistance, low density, and flexibility.

Previously, HDPE mixed conducting polymer composites were fabricated by mixing the HDPE matrix with different types of conducting fillers.[16,17,24–27] Tjong et al.[16] analyzed the AC and DC conductivities of HDPE-carbon nanofiber (CNF) composites in the frequency range of 100 Hz to 10 MHz and composites followed the scaling law of percolation theory and ϕ_c of the composites was 0.97 vol % of CNF. Yang et al.[17] performed the dielectric analysis of vapor grown carbon nanofiber (VGCNF) reinforced HDPE composites in the frequency range

Correspondence to: S. H. Park (spark@jnu.ac.kr) and J. O. Park(jop@jnu.ac.kr).

Contract grant sponsor: Korea Ministry of Knowledge Economy (Grant-in-Aid for Strategy Technology Development Programs); contract grant number: 10030037.

of 0.01–10^5 Hz in the temperature range of 35–120°C, and the dielectric properties of VGCNF-HDPE composites followed the percolation theory and ϕ_c value for permittivity and loss factor was 15 wt % of VGCNF. Huang et al.[24] studied the electrical and dielectric properties of polyethylene-aluminum (Al) composites and they applied DC conductivity and dielectric properties to the percolation theory and found that ϕ_c of the composites was 24 wt % of Al. Bischoff et al.[25] studied the effects of electrical conductivity, AC conductivity and positive temperature coefficient (PTC) of carbon black-HDPE composites. The percolation theory was applied to the DC conductivity, and the value of composites was found to be 0.1 volume fraction of carbon black. AC conductivity was also analyzed with frequency at different temperatures. Wang et al.[26] analyzed the impedance spectra of carbon black filled HDPE composites and analyzed the conductivity by percolation theory. The ϕ_c of the composites was 20% of carbon black. Panwar et al.[27] analyzed DC conductivity, resistivity with temperature of HDPE-Gr composites. That is, the dielectric constant and loss factor from 20 Hz to 5 MHz and EMI SE measurements in the frequency range of 8.0–12.0 GHz using a microwave bench were measured.

However, there is no report on the dielectric analysis of HDPE-Gr composites in the radio frequency region and the percolation theory analysis of AC conductivity of HDPE-Gr composites according to lower frequency region. In this article, we analyzed the dielectric constant, AC conductivity and loss factor of HDPE-Gr composites in the lower frequency (20 Hz to 10^5 Hz) and the radio frequency range (1 MHz to 3 GHz). In the lower frequency range, the percolation theory was applied to analyze to dielectric constant and AC conductivity according to graphite volume fraction as well as frequency. The EMI SE of composites in radio frequency range was calculated. The HDPE-Gr composites were prepared by mixing and the hot compression mold technique. The composites consisted of HDPE as the insulating polymer matrix and graphite as the conducting filler. As a linear polymer, HDPE has no branching and has a more closely packed structure with higher density, higher chemical resistance, and harder temperatures resistance (120°C for short periods, 110°C continuously) than LDPE. Owing to these specific properties of HDPE, HDPE-Gr conducting polymer composites can be applied as charge storing capacitors, decoupling capacitors, and EMI shielding materials.

EXPERIMENTAL

Materials

The matrix polymer used in this work is a commercial grade (F41 003) HDPE resin with granules, manufactured by Indian Petrochemicals, Vadodara, Gujrat, India. The various physical parameters of HDPE are as follows: color = transparent, density = 0.96 g/cm^3, hardness shore $D = \sim 75$, melt flow = 5 to 18 g/10 min, melting temperature = 130°C, vicat softening temperature = 125°C, heat deflection temperature = 90°C, molecular weight = 50,460, dielectric constant at 1 MHz = 2.2–2.35, dissipation factor at 1 MHz = 1×10^{-4} and volume resistivity = 1×10^{13} Ω cm. As the electrical conducting filler, graphite powder with average particle size ranging from 10 to 20 μm was used (supplied by Graphite India). Some of the properties of graphite are as follows: color is black, density = 1.75 g/cm^3, maximum usable temperature = 3600, modulus of elasticity (Young modulus) = 4.8 GPa, electrical resistivity = 7.5×10^{-5} Ω cm and carbon-graphite% = 30–70.

Composite sample preparation

The HDPE granules were ground to obtain fine particles (212–250 μm) using Aurther H. Thomas type Willey Grinder. The polymer and filler powders were tumble mixed thoroughly for 4 h in a glass beaker with a magnetic stirrer.[27,28] The speed of the magnetic stirrer was maintained around 400 rpm without any heating. This process coated the conducting graphite powder on the surface of the HDPE particles, so it is referred to as prelocalization of the conductive phase. Prolonged mixing improved the homogeneity of the spatial distribution of the conductive particles and their uniform coating thickness on the HDPE particles. The tumble mixed prelocalized powders was prepared for different graphite contents in the range i.e., 0, 3, 5, 7, 10, 15, 20, 25, and 30 wt % of graphite under similar conditions. The corresponding volume fractions of Gr (ϕ) of these samples were 0, 0.016, 0.0274, 0.039, 0.056, 0.086, 0.099, 0.118, and 0.187.

By using a hydraulic press (Shimadzu, Kyoto, Japan) of ram diameter 42.7 mm, the graphite coated HDPE powder was initially pressed for 5 min at room temperature to eliminate any void formation within the pellet. By using a rectangular mold, rectangular specimens of length 2.28, width 1.01 cm and thickness ~ 0.2 to 0.25 were obtained. The processing temperature (initial temperature) and the pressure in the molding procedure are the main concerns in the fabrication of graphite mixed polymer composite pellets. The composites should have good conductivity as well as hardness. After the fabrication procedures were setup, all the samples were prepared at processing temperature of 100°C under 70 MPa and baked at 115 °C (below a melting temperature) for 15 min at atmosphere pressure. After baking the samples, all the samples were cooled down to room temperature at atmospheric pressure

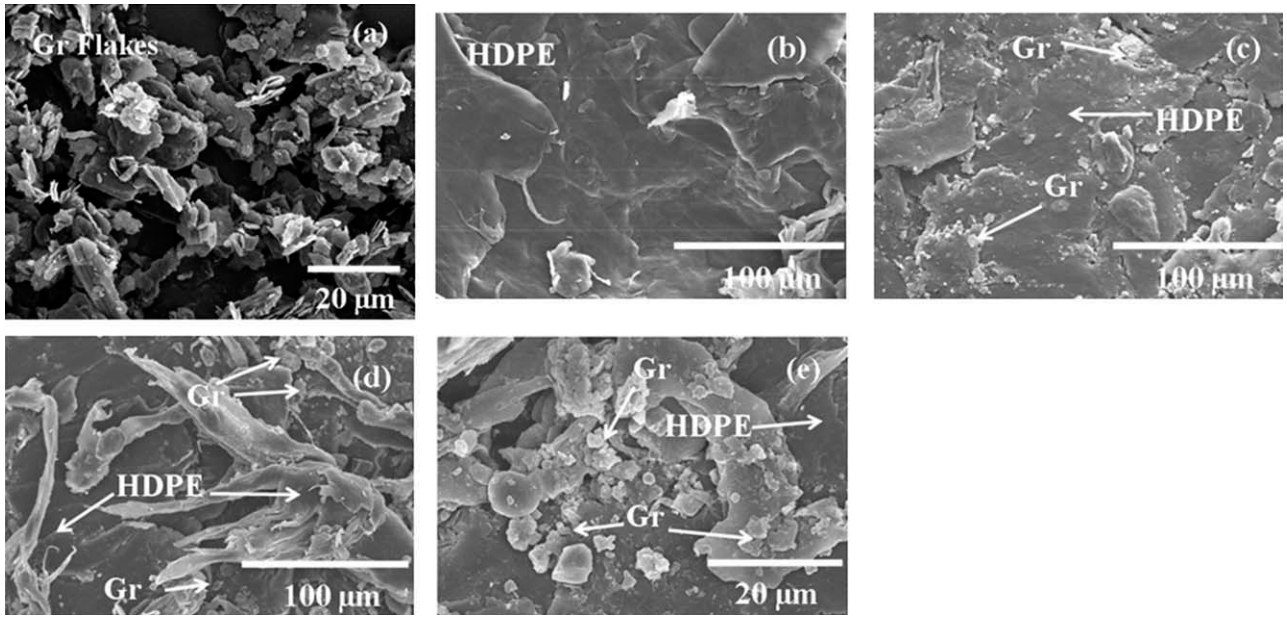

Figure 1 Scanning electron microscopy (SEM) images of (a) graphite flakes at ×1000 magnification, (b) surface part of hot compressed mold pure HDPE sample at ×500 magnification, (c) surface part of composite with $\phi = 0.039$ (7 wt %) at ×500 magnification, (d) surface part of composite with $\phi = 0.086$ (15 wt %) at ×500 magnification and (e) surface part of composite with $\phi = 0.086$ at ×2000 magnification.

to eliminate porosity, bubbles or blisters. This procedure improves the electrical properties, minimizes the after-shrinkage and enhances the quality and appearance of the samples. The specimens were taken out from the mold and the surfaces of the specimens were polished by sandpaper to remove the polymer rich surface layer and to eliminate surface irregularities. The specimens were sealed in air free polyethylene bags prior to measurements to avoid atmospheric and humidity effects that may induce some changes in the conductivity of the specimens.

Characterization

Scanning electron microscopy

Scanning electron microscopy (SEM) of the HDPE-Gr composites was performed using a Hitachi scanning electron microscope (Model No. *S*-4700). All the samples were gold sputtered prior to measurement.

Measurements

For the measurement of resistance, both opposite surfaces of the samples were coated with SEM grade conductive silver paint. The resistance of the samples having resistance less than 200 $M\Omega$ was measured using a conventional digital multi-meter. When the resistance exceeded 200 $M\Omega$, a Keithley Pico ammeter was used to measure the resistance.

For studying the dielectric properties, the capacitance (C) and dissipation factor ($\tan\delta$) of the samples were measured in two frequency ranges, 20 Hz to 5 MHz and 1 MHz to 3 GHz, by using a Hewlett–Packard (HP) Impedance Analyzer (Model No. 4294) and RF Impedance/Material Analyzer (Model No. E-4991 A), respectively. The dielectric constant (ε') of composites is calculated from the formula $\varepsilon' = Ct/\varepsilon_0 A$ (,) where ε_0 is the permittivity of the free space, t is the thickness, A is the area, and C is the capacitance.

RESULTS AND DISCUSSION

Morphology

Figure 1(a) shows the SEM image of the graphite particles at ×1000 magnification which have a flaky shape.[27,28] Figure 1(b) shows the SEM image of surface part of pure HDPE sample after compression molding. This image corresponds to the formation of solid HDPE. Figure 1(c,d) show the SEM images of surface part of composites at ϕ_c and above ϕ_c having graphite volume fraction $\phi = 0.039$ (7 wt %) and 0.086 (15 wt %), respectively. From Figure 1(b–d), SEM images of samples were executed at ×500 magnification. Figure 1(e) shows the SEM images of composite having $\phi = 0.086$ (15 wt %) at higher magnification (×2000). Figure 2(a–c) show the SEM images of cross section part of pure HDPE, composites having $\phi = 0.039$ (7 wt %) and 0.086 (15 wt %). From Figure 2(a–c), SEM images of samples were also executed at ×500 magnification. In Figure 1(c–e) and Figure 2(b,c), the HDPE and graphite zones

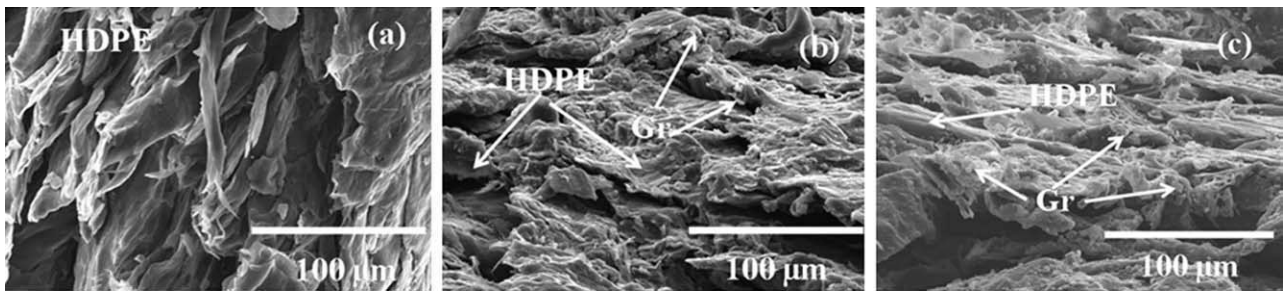

Figure 2 Scanning electron microscopy (SEM) images of (a) cross section part of hot compressed mold pure HDPE sample at ×500 magnification, (b) cross section part of composite with $\phi = 0.039$ (7 wt %) at ×500 magnification and (c) cross section part of composite with $\phi = 0.086$ (15 wt %) at ×500 magnification.

have been specified by white arrow. From the figures, it is clear that the presence of graphite particles (flakes type) can be seen between the interfacial regions of the HDPE matrix with the addition of graphite.

Dielectric properties in low frequency range

Conducting polymer composites possess a frequency (ω) dependent, complex dielectric constant $\varepsilon^*(\omega) = \varepsilon'(\omega) - i\varepsilon''(\omega)$. The real part $\varepsilon'(\omega)$ represents the relative dielectric constant and the imaginary part $\varepsilon''(\omega)$ accounts for the dielectric loss. The ratio of the imaginary to the real part ($\varepsilon''/\varepsilon'$) is the "dissipation factor," which is represented by tan δ, where δ is called as the "loss angle" denoting the angle between the voltage and the charging current. To investigate the dielectric behavior of HDPE-Gr composites in the low frequency (f_L) range, the room temperature ε' and tan δ of the composite were calculated in the frequency range from 20 Hz to 100 kHz.

Figure 3 shows the variation of ε' of HDPE-Gr composites as a function of φ of Gr at 50 kHz. The ε' of HDPE-Gr increases with the increasing volume fraction of Gr and enhances greatly near $\phi = 0.039$. This enhancement of ε' in the neighborhood of the percolation threshold is also predicted by the power law[29–31] as follows:

$$\varepsilon' \propto (\phi_c - \phi)^{-s} \tag{1}$$

where ϕ_c is the critical filler volume fraction at which percolation in ε' takes place and it is called percolation threshold, and s is a critical exponent of ε'. The log-log plots of eq. (1) are shown in the inset of Figure 3. The best fit of the ε' data to the log-log plots of eq. (1) gives $\phi_c = 0.040$, which is near equal to the experimental threshold value ($\phi_c = 0.039$) of the composites. The value of s is found to be 0.76, which is close to the normal value given by percolation theory.[29]

The dependence of ε' of the HDPE-Gr composites on the low frequency (f_L) is shown in Figure 4. When $\phi < \phi_c$, for example at $\phi < 0.039$, the ε' of the composites exhibited weaker frequency dependence, but when $\phi \geq \phi_c$, ε' of the composites exhibited stronger frequency dependence. The Gr filled HDPE

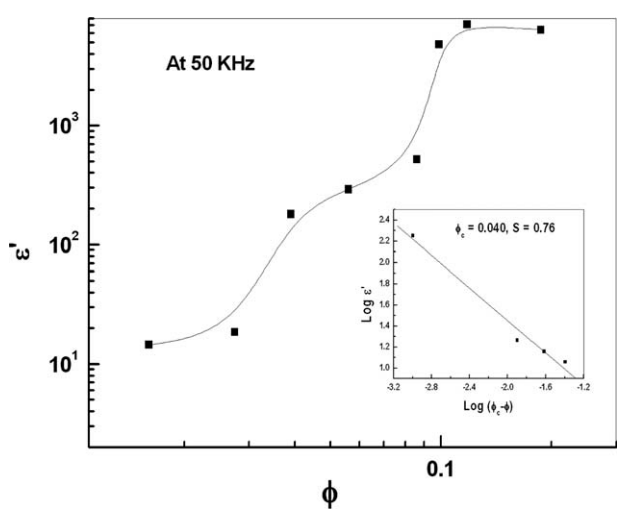

Figure 3 ε' of HDPE-Gr composites as a function of φ at 50 kHz. Inset 3 Plot of log ε' versus log ($\phi_c - \phi$) of HDPE-Gr composites.

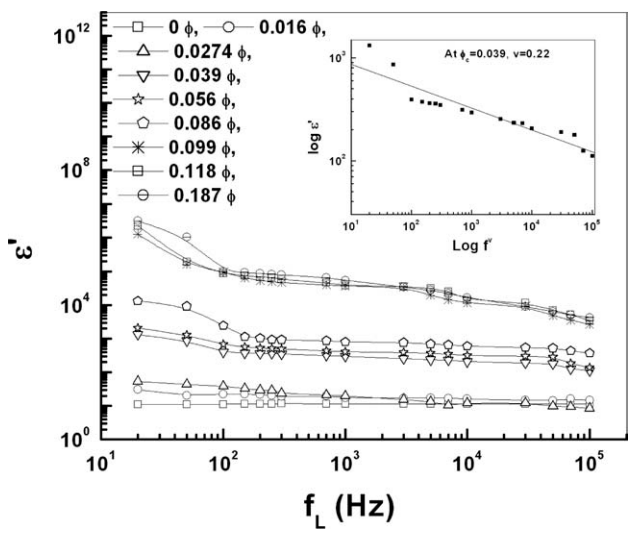

Figure 4 Variation of ε' of the HDPE-Gr composites as a function of f_L for different φ. Inset 4 log-log plot of ε' versus f_L at ϕ_c.

composites depict large value of ε′ at lower frequencies while the value of ε′ decreased at higher frequencies. At low frequencies, the polarization follows the change of the electric field. In this case, highest value of ε′ is obtained. At high frequencies, the electric field changes too fast for the polarization effects to appear. In this case, lowest value of ε′ is obtained.[28] From the figure, it is clear that the values of ε′ of composite increased with increasing ϕ. The increment in ε′ of composite with addition of ϕ (Gr content) could be mainly ascribed to following two reasons.[20] One reason is Maxwell-Wagner (MW) interfacial polarization originating in the insulator-conductor (HDPE-Gr) interfaces. Another reason is due to the formation of mini-capacitor networks in the HDPE-Gr composites with increasing Gr content. Large enhancement in ε′ of composites in the low frequency region occurs due to the Maxwell-Wagner polarization originating in the insulator-conductor interfaces.[28,32,33] The high value of $\varepsilon' = 3.12 \times 10^6$ was observed at 20 Hz for the composites with $\phi = 0.187$. High value of ε′ could be used in capacitor applications.

The frequency variation of ε′ at $\phi \sim \phi_c$ as predicted by percolation theory[29] is

$$\varepsilon'(f, \phi_c) \propto f_L^{-v} \tag{2}$$

where v is the critical exponent. The log–log plot of eq. (2) is shown in the inset of Figure 4. From the data, the value of v was 0.22.

The dependence of tan δ of the HDPE-Gr composites on low frequency (f_L) is shown in Figure 5. Except for the composites with $\phi = 0$ and 0.16, tan δ of all the composites increased up to 150 Hz and thereafter, its value decreased with increasing frequency. This is because the induced charges gradually fail to follow the reversing field causing a reduction in the electronic oscillations as the frequency is increased.[28] From the figure, it is clear that the values of tan δ increased with increasing ϕ. In the lower frequency region, the tan δ increase sharply for the composites having $\phi \geq \phi_c$. Large increment of tan δ in lower frequency region may be attributedto the interfacial polarization mechanism of the heterogeneous system. The high value of tan $\delta = 5.58 \times 10^4$ was observed at 150 Hz for the composites with $\phi = 0.086$. High values of tan δ of the composites could be utilized for decoupling capacitor applications. Due to the Maxwell-Wagner polarization effect in the HDPE-Gr composites systems, the ε′ and tan δ of HDPE-Gr composites system was found to be higher than other composite systems.[34,35]

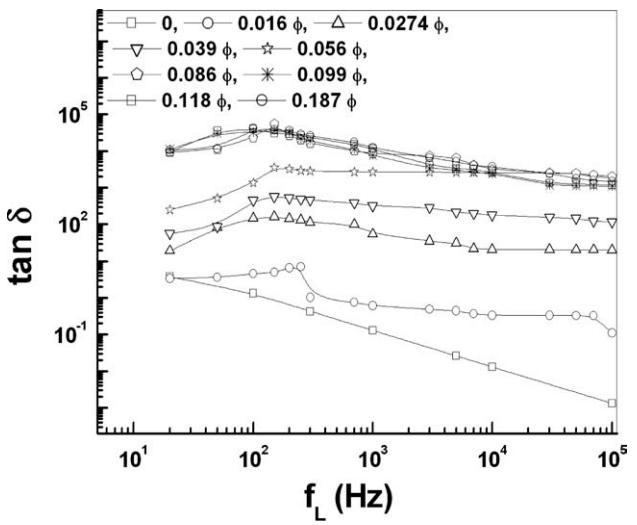

Figure 5 Variation of tan δ of the HDPE-Gr composites as a function of f_L for different ϕ.

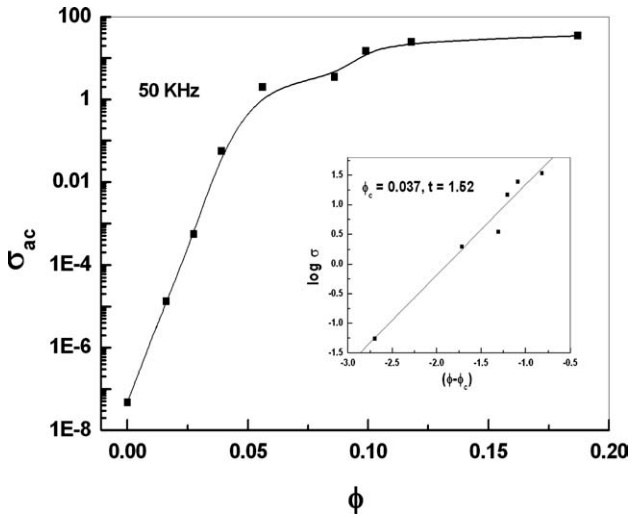

Figure 6 σ_{ac} of HDPE-Gr composites as a function of ϕ at 50 kHz. Inset 6 Plot of log σ versus log $(\phi - \phi_c)$ of HDPE-Gr composites.

Figure 6 shows the variation of the AC conductivity (σ_{ac}) of the HDPE-Gr composites as a function of ϕ of Gr at 50 kHz. The σ_{ac} of composites is calculated from the formula $\sigma_{ac} = \omega_L \varepsilon_0 \varepsilon'$ tan δ, where $\omega_L = 2\pi f_L$. In this formula, ω_L is the angular frequency, f_L is ordinary frequency and ε_0 is the dielectric constant of vacuum. The σ_{ac} of the composites increased with the increasing volume fraction of Gr, and the insulator–conductor transition of composites was found near to $\phi = 0.039$ (7 wt %). According to classical percolation theory, the conductivity of composites near the insulator-conductor transition can be represented by the power law model of percolation theory[36–38]:

$$\sigma_{ac} \propto (\phi - \phi_c)^t \tag{3}$$

where ϕ_c is the critical filler volume fraction at which percolation in σ_{ac} takes place, and t is the

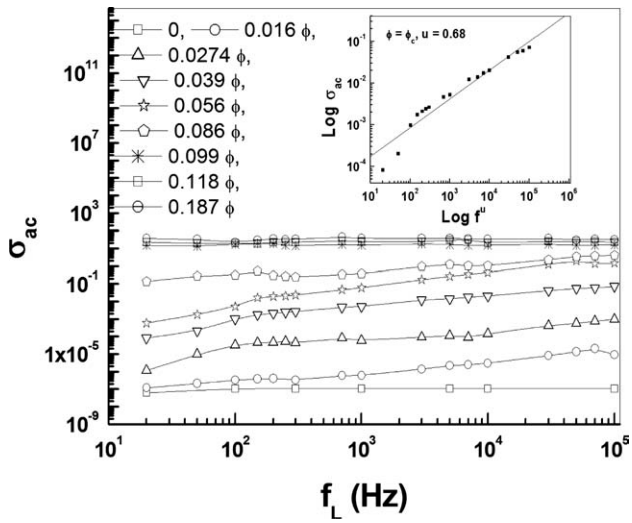

Figure 7 Variation of σ_{ac} of the HDPE-Gr composites as a function of f_L for different ϕ. Inset 7 log-log plot between σ_{ac} and f_L of the HDPE-Gr composites at ϕ_c.

critical exponent of conductivity. The experimental values of σ_{ac} were fitted to eq. (3) and a log-log plot of the power law was generated, as shown in the inset of Figure 6. The best fit of the conductivity data to the log-log plots of the power law gives $\phi_c = 0.037$ ($\sim$ 7wt %) and $t = 1.52$. The value of t for our composite system was found to be less than to 2, which is a universal value of three dimensional (3-D) systems which is a geometrical phase transition. The universal value of $t = 2$ is found to be applicable for touching particle model in which physical contact between the conducting particles is necessary to make a percolative path while Kirkpatrick[39] analyzed percolation theory and proved theoretically that t is a universal constant which is independent of the chemical natures and geometries of the constituents. The value of $t = 1.6$ has been predicted by[39,40] for 3-D system while computer simulations give $t = 2.0$.[37] Therefore, value of t in our composite system is near to values of t obtained by[39,40] for 3-D systems. The reason of deviation of t from universal value ($\sim$ 2) has also been reported by previous research articles.[41–43] It was reported[41,42] that the theoretical model does not consider the interaction between conducting particles and conducting particle and polymer matrix. They concluded that theoretically if physical contact is not necessary (i.e., charge can tunnel through the barrier) to make the percolative network, nonuniversal value of t can be obtained for composite systems. Research article[43] reported that the value of t depends on the authors and type of simulation used for fitting the eq. (2). The best linear fitting to the eq. (2) is obtained by varying the value of ϕ_c and different value of t is obtained with different ϕ_c.

The dependence of σ_{ac} of the HDPE-Gr composites on f_L is shown Figure 7. As we have discussed in Figure 6, it is clear that σ_{ac} depends onε', tan δ and f_L. After calculating σ_{ac} in low frequency range for each composite, graph was plotted between σ_{ac} with f_L. A small value of ac conductivity increased with the increase of frequency for the composites with $\phi = 0.0$ to 0.086 while σ_{ac} of composites with $\phi = 0.099$ to 0.187 remained constant with the increase of frequency. So, the composites with $\phi = 0.099$ to 0.187 have high σ_{ac} and weak frequency dependence, and these properties of the material could be utilized as antistatic media and shielding for EMI or RFI of electronic devices. The frequency variation of σ_{ac} at $\phi \sim \phi_c$ as predicted by percolation theory[29] is

$$\sigma_{ac}(f, \phi_c) \propto f_L^u \tag{4}$$

where u is the critical exponent. The log–log plot of eq. (4) is shown in the inset of Figure 7. From the data, the value of u was 0.68, which is slightly lower than the universal one ($u = 0.70$).[29] The critical exponents u and v are related as $u + v = 1$. In the present case, $u = 0.68$ and $v = 0.22$ i.e., $u + v = 0.9$, which is close to the normal value given by percolation theory. The above analysis confirmed the percolation phenomenon in the HDPE-Gr composites.

Dielectric properties in the high frequency region

To investigate the dielectric behavior of the HDPE-Gr composites at high frequencies (f_H), the room temperature ε' and tan δ of the composites were calculated in the frequency range from 1 MHz to 3 GHz (radio frequency). Figure 8 shows the ε' of the composites as a function of f_H for various contents of graphite. A small variation in ε' was observed for the composites with $\phi \leq \phi_c = 0.039$ (7 wt %) and a large variation was observed for the composites

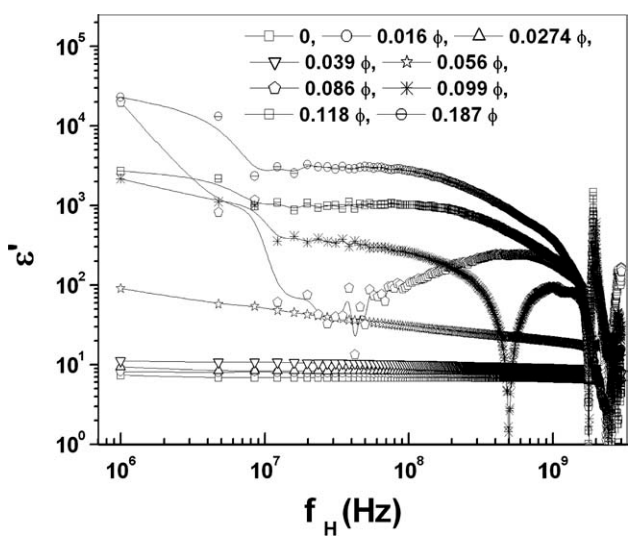

Figure 8 Variation of ε' of the HDPE-Gr composites as a function of f_H for different ϕ.

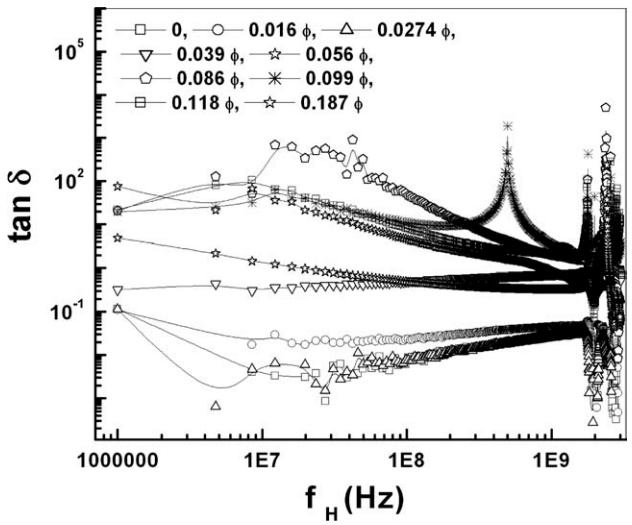

Figure 9 Variation of tan δ of the HDPE-Gr composites as a function of f_H for different ϕ.

with $\phi \geq \phi_c$ from 1 MHz to GHz. The ε′ of the composites with ϕ = 0.086 and 0.099 shows complex fluctuations at the measured f_H = 0.002 GHz to 3 GHz. The maximum values of $\varepsilon' = 2.3 \times 10^4$ was obtained at 1 MHz for the composites with ϕ = 0.187 (30 wt %) and in the GHz frequency range, the maximum values of $\varepsilon' = 1.54 \times 10^3$ was obtained at 1.86 GHz for the composite with ϕ = 0.118. The HDPE-Gr composites attained higher values of dielectric constant with higher graphite content in HDPE-Gr composites due to the formation of mini-capacitor networks in the HDPE-Gr composites with increasing Gr content. High values of ε′ in the radio frequency range are useful in EMI SE applications.

Figure 9 shows the tan δ of the HDPE-Gr composite as a function of f_H for various contents of graphite. The tan δ for composites with ϕ = 0, 0.16, 0.027, 0.086, 0.099, 0.118, and 0.0187 shows a complex fluctuation with the measured f_H. And, the tan δ of the composites with ϕ = 0.039 increases with increasing frequency while tan δ of the composite with ϕ = 0.056 decreases with increasing frequency, although tan δ shows complex variation above 1 GHz for both composites. The maximum value of tan $\delta = 4.9 \times 10^3$ is obtained at 2.4 GHz for the composite with ϕ = 0.086 (15 wt %). High values of tan δ in the radio frequency range are useful in EMI SE applications. The noise in the values of ε′ and tan δ is observed near to 0.5–3 GHz due to the oscillation of ε′ and tan δ in this frequency ranges.

Figure 10 shows the σ_{ac} of the HDPE-Gr composites as a function of f_H (radio frequency) for various contents of graphite. σ_{ac} increases sharply with the increase of f_H for composites with ϕ = 0 to 0.056 but a complex fluctuation of σ_{ac} is seen when $f_H \geq 1$ GHz. For composites with ϕ = 0.086 to 0.187, σ_{ac} is high and remains constant with the increase of the frequency, although σ_{ac} shows complex fluctuation when $f_H \geq 1$ GHz. Because the HDPE-Gr composites with ϕ = 0.086 to 0.187 have high σ_{ac} and weak frequency dependence in radio frequency range, they can be utilized in EMI or RFI shielding of electronic devices.

EMI shielding

An electromagnetic shield is a conductive material which attenuates electromagnetic energy. The total shielding effectiveness (SE_T) is defined as the ratio of incident to transmitted power and which is equal to SE due to absorption of EM energy, SE due to reflection of EM energy from the material surface and multiple internal reflection of EM radiation. Therefore, the total SE_T of the sample is expressed as eq. (5)[44–46]:

$$SE_T = 10 \log \left(P_{in}/P_{out} \right) = SE_A + SE_R + SE_I, \quad (5)$$

where P_{in} and P_{out} are the power incident on and transmitted through a shielding material, respectively. The SE_T is expressed in decibels (dB). SE_A and SE_R are the absorption and reflection (from both sides of the material with neglect of the multiple reflections inside the barrier) shielding efficiencies, respectively. The third term (SE_I) is a positive or negative correction term induced by the reflecting waves inside the shielding barrier, negligible when $SE_A > 15$ dB. The terms in eq. (5) can be described as

$$SE_A = 8.86 \alpha l \quad (6)$$

$$SE_R = 20 \log \frac{|1+n|^2}{4|n|} \quad (7)$$

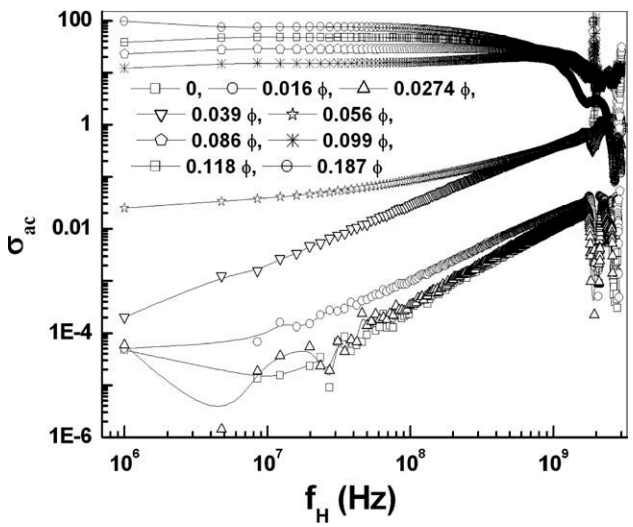

Figure 10 Variation of σ_{ac} of the HDPE-Gr composites as a function of f_H for different *f*.

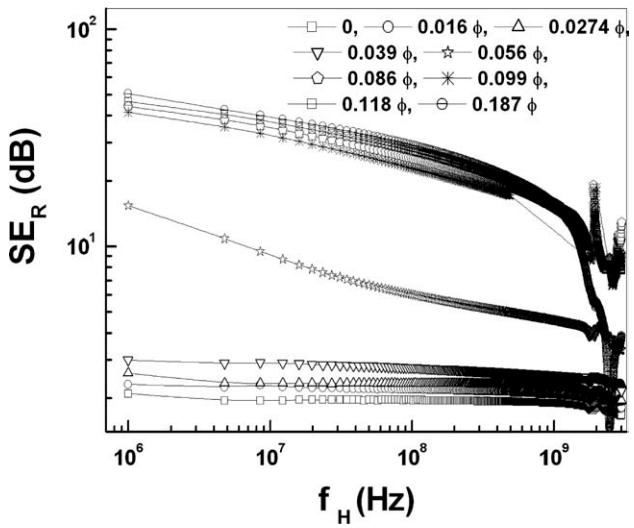

Figure 11 Variation of SE_R of the HDPE-Gr composites as a function of f_H for different ϕ.

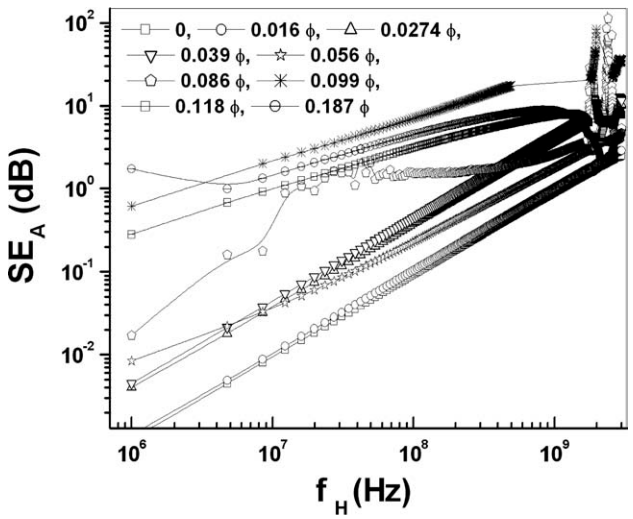

Figure 12 Variation of SE_A of the HDPE-Gr composites as a function of f_H for different ϕ.

$$SE_I = 20 \log \left| 1 - \frac{\exp(-2\gamma l)(1-n)^2}{(1+n)^2} \right| \quad (8)$$

where the parameters α, n, and γ are defined by the following equations, and l is the thickness of the shielding barrier.

$$\alpha = \frac{2\pi}{\lambda_0} \sqrt{\frac{\varepsilon' \sqrt{1+\tan^2\delta}}{2}} \quad (9)$$

$$n = \sqrt{\frac{\varepsilon'\left(\sqrt{1+\tan^2\delta} \pm 1\right)}{2}} + i\sqrt{\frac{\varepsilon'\sqrt{1+\tan^2\delta} \mp 1}{2}} \quad (10)$$

$$\gamma = \left(\frac{2\pi}{\lambda_0}\right)\sqrt{\frac{\varepsilon'\sqrt{1+\tan^2\delta} \mp 1}{2}} + i\left(\frac{2\pi}{\lambda_0}\right)\sqrt{\frac{\varepsilon'\left(\sqrt{1+\tan^2\delta} \pm 1\right)}{2}} \quad (11)$$

where λ_0 is the wave length, ε' the real part of complex relative permittivity, the $\pm$ and $\mp$ signs are applied for positive and negative ε', respectively.

Using eqs. (6), (7), (9), and (10) and the values of ε' and $\tan\delta$ in the frequency range from 1 MHz to 3 GHz, the values of SE_R and SE_A for the HDPE-Gr composites were calculated. The SE_R and SE_A of the composites as a function of f_H (1 MHz to 3 GHz) are shown in Figures 11 and 12, respectively. The SE_R of the composites with $\phi \leq \phi_c$ decreases slowly with the increase of f_H except when oscillations occur above 1 GHz while the SE_R of the composites with $\phi > \phi_c$ shows large variation with the increase of f_H except when oscillations occur above 1 GHz. The SE_R of the composites increases with the increase of ϕ. A high value ($\sim$ 50.44 dB) of SE_R is obtained at 1 MHz for the composites with $\phi = 0.187$ (30 wt %) because these composites have high values of ε' and $\tan\delta$. The SE_A of HDPE-Gr composites increase with f_H because SE_A is directly proportional to f_H as observed by eqs. (6) and (9). The maximum value (114.11 dB) of SE_A is obtained at 2.46 GHz for composites with $\phi = 0.086$ (15 wt %).

Using eqs. (8) and (11), the values of SE_I were calculated. The SE_I of the composites with $\phi = 0$ to 0.056 was evaluated and it is shown in Figure 13 while SE_I of the composites with $\phi = 0.086$ (15 wt %) to 0.187 (30 wt %) was 0.

Using eq. (5), the SE_T of the composites was calculated by adding SE_R, SE_A and SE_I. The SE_T of the composites as a function of f_H is shown in Figure 14. The SE_T of the composites increases with increasing ϕ and decreases with increasing f_H except when

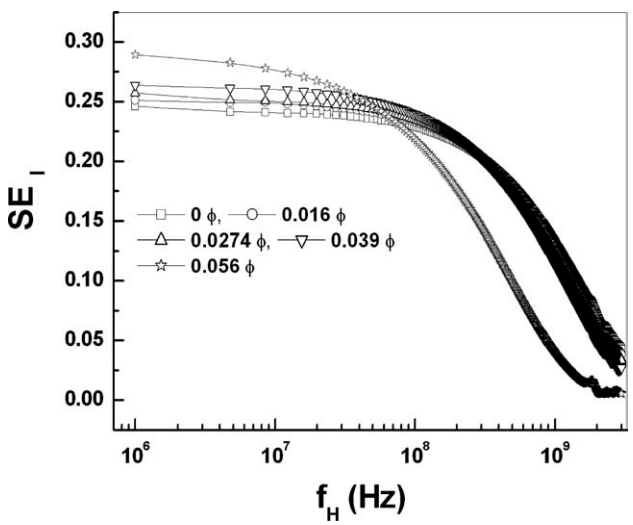

Figure 13 Variation of SE_I of the HDPE-Gr composites as a function of f_H for different ϕ.

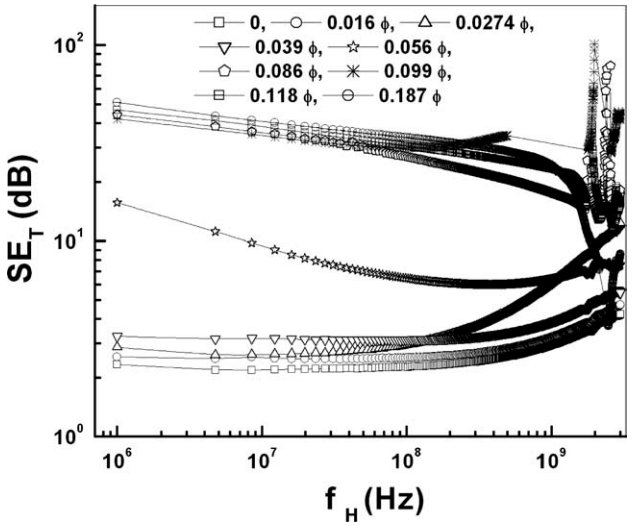

Figure 14 Variation of SE_T of the HDPE-Gr composites as a function of f_H for different ϕ.

oscillations occur above the 1 GHz. As expected from the above data on SE_R, SE_A and SE_I, the trendof SE_T shows that SE_R comprises a major portion of the EMI SE. The maximum value (101.42 dB) of SE_T is obtained at 1.97 GHz for the composites with $\phi = 0.099$ (20 wt %). The high value of EMI SE can be utilized for shielding various types of equipment from electromagnetic interference in the radio frequency range.

CONCLUSION

In this article, dielectric properties of HDPE-Gr composites in low and radio frequency ranges have been analyzed. Both dielectric constant and AC conductivity of HDPE-Gr composites followed the power law model of percolation theory at the percolation threshold $\phi_c \sim 0.039$. At $\phi = \phi_c$, the dielectric constant and AC conductivity of HDPE-Gr composites at low frequencies followed the power law model of percolation theory. The dielectric constant of HDPE-Gr composites with $\phi > \phi_c$ was strongly frequency (low and high) dependent. The highest dielectric constant (3.12×10^6) was obtained at 20 Hz for composites with $\phi = 0.187$. These composites can be used in charge storing devices. The highest dissipation factor (5.58×10^4) was obtained at 150 Hz for composites with $\phi = 0.086$, which makes these composites suitable for decoupling capacitor applications. Above $\phi \geq 0.086$, the composites possessed high values of AC conductivity and exhibited weak frequency (low and high) dependence, so these composites can be utilized as antistatic media and in EMI shielding applications. The main contribution of these composites to effective EMI shielding was due to reflection. The maximum value (101.42 dB) of SE_T was obtained at 1.97 GHz for composites with $\phi = 0.099$. Finally, the proposed HDPE-Gr composites exhibited a high dielectric constant and dissipation factor with the addition of graphite content in the low and radio frequency ranges, and the composites with high graphite filler had high EMI shielding effectiveness in radio frequency range, so these composites can be utilized in charge storing capacitors, decoupling capacitors, and electromagnetic interference shielding applications.

References

1. Celzard, A.; Mcrae, E.; Furdin, G.; Mareche, J. F. J Phys Codens Mater 1997, 9, 2225.
2. Panwar, V.; Park, J. O.; Park, S. H.; Kumar, S.; Mehra, R. M. J Appl Polym Sci 2010, 115, 1306.
3. Zheng, Q.; Song, Y.; Wu, G.; Yi, X. J Polym Sci Part B Polym Phys 2001, 39, 2833.
4. Krupa, I.; Novak, I.; Chodak, I. Synth Met 2004, 145, 245.
5. Lee, G. J.; Suh, K. D.; Im, S. S. Polym Eng Sci 1998, 38, 471.
6. Chodak, I.; Krupa, I. J Mater Sci Lett 1999, 18, 1457.
7. Yang, G.; Tang, R.; Xiao, P. Polym Compos 1997, 18, 477.
8. Nakamura, S.; Saito, K.; Sawa, G.; Kitagawa, K. Jpn Appl Phys 1997, 36, 5163.
9. Huang, X. Y.; Jiang, P. K.; Kim, C. U. J App Polym Sci 2007, 102, 124103.
10. Dang, Z. M.; Zhang, Y.; He.; Tjong, S. C. Synth Met 2004, 146, 79.
11. Mclachlan, D. S.; Chiteme, C.; Park, C.; Wise, K. E.; Lowther, S. E.; Lillehei, P. T.; Siochi, E. J.; Harrision, J. S. J Polym Sci Part B Polym Phys 2005, 43, 3273.
12. Barrau, S.; Demont, P.; Peigney, A.; Laurent, C.; Colette, L. Macromolecules 2003, 36, 5187.
13. Xi, Y.; Yamanaka, A.; Bin, Y.; Masaru, M. J Appl Polym Sci 2007, 105, 2868.
14. Bai, Y.; Cheng, Z. Y.; Bharti, V.; Xu, H. S.; Zhang, Q. M. Appl Phys Lett 2000, 76, 3804.
15. Rao,Y.; Wong, C. P. J Appl Polym Sci 2004, 92, 2228.
16. He, L. X.; Tjong, S. C. Eur Phys J E 2010, 32, 249.
17. Yang, S.; Benitez, R.; Fuentes, A.; Lozano, K. Compos Sci Technol 2007, 67, 1159.
18. Heaney, M. B. Appl Phys Lett 1996, 69, 2602.
19. Strumpler, R. J Appl Phys 1996, 80, 6091.
20. Chen, Q.; Du, P.; Lu, J.; Weng, W.; Han, G. Appl Phys Lett 2007, 91, 22912.
21. Lu, J.; Moon, K. S.; Xu, J.; Wong, C. P. J Mater Chem 2006, 16, 1543.
22. Chung, D. D. L. Carbon 2001, 39, 279.
23. Wu, J.; Chung, D. D. L. Carbon 2002, 40, 445.
24. Huang, X. Y.; Jiang, P. K.; Kim, C. U. J Appl Phys 2007, 102, 124103.
25. Bischoff, M. H.; Oise, F.; Dolle, E. Carbon 2001, 39, 375.
26. Wang, Y. J.; Pan, Yi.; Zhang X. W.; Tan, K. J Appl Polym Sci 2005, 98, 1344.
27. Panwar, V.; Mehra, R. M. Polym Eng Sci 2008, 48, 2178.
28. Panwar, V.; Sachdev, V. K.; Mehra, R. M. Eur Polym Mater 2007, 43, 573.
29. Nan, C. W. Prog Mater Sci 1993, 37, 1.
30. Chiteme, C.; McLachlan, D. S. Phys Rev B 2003, 67, 24206.
31. Bergman, D. J Phys Rev Lett 1980, 44, 1285.
32. Foulger, S. H. J App Polym Sci 1999, 72, 1573.
33. Meakins, R. J. Progress in Dielectrics; Wiley: New York, 1961, p 151.

34. Roy A. S.; Anilkumar, K. R.; Prasad, M.V. N. A. J Appl Polym Sci 2011, 121, 675.
35. Dang, Z. M.; Shen, Y.; Nan, C.W. Appl Phys Lett 2002, 81, 4814.
36. Panwar, V.; Mehra, R. M. Eur Polym Mater 2008, 44, 2367.
37. Stauffer, D.; Aharony, A. Introduction to Percolation Theory; Taylor & Francis: London, 1992, p 89.
38. Efros, A. L.; Shklovskii, B. I. Phys Stat Sol 1976, 76, 475.
39. Kirkpatrick, S. Rev Mod Phys 1973, 45, 574.
40. Medalia, A. I. Rubber Chem Technol 1986, 59, 432.
41. Balberg, I. Phys Rev Lett 1987, 59, 1305.
42. Wu, J.; McLachlan, D. S. Phys Rev B 1997, 56, 1236.
43. Kilbride, B. E.; Coleman, J. N.; Fraysse, J.; Fournet, P.; Cadek, M.; Drury, A.; Roth, S.; Hutzler, S. B.; Blau, W. J. J Appl Phys 2002, 92, 4024.
44. Liu, Z.; Bai, G.; Huang, Y.; Ma, Y.; Du, F.; Li, F.; Guo, T.; Chen, Y. Carbon 2007, 45, 821.
45. Joo, J.; Epstein, A. J Appl Phys Lett 1994, 65, 2278.
46. Schulz, R. B.; Plantz, V. C.; Brush, D. R. IEEE Trans 1988, 30, 187.